

Nuclear Wobbling Motion

Emma Suckling*

URN: 3531961

February 12, 2006

Abstract

The basic theory of rotational motion in nuclei was reviewed with aim to understanding the concepts of wobbling motion. An existing piece of computer code was used based on the exact diagonalisation of a perturbed Hamiltonian, to generate results on nuclear wobbling motion. The code calculated the energy eigenvalues, K -eigenvalue (where K is the eigenvalue of the quantised first angular momentum component, \hat{I}_1) and probability for rotations to be aligned along the first axis for a rigid body and irrotational flow structure. This was achieved by solving the Schrodinger equation then using a standard mathematical function to diagonalise the Hamiltonian matrix.

Energy spectra were produced exhibiting anharmonicity similar to those described by the experimental data published in 2001 for Lu isotopes. However, only the collective properties of the nucleus were considered by the model, so direct comparisons cannot be made until it is extended to account for microscopic properties such as pairing, spin dependence and other shell effects.

*University of Surrey, Guildford, GU2 7XH. UK

Contents

1	Introduction	3
2	Background Theory	5
2.1	Rotational Motion	5
2.2	Deformation Parameters	5
2.3	Moment Of Inertia	6
2.4	Macroscopic Quantum Rotations	7
2.5	The Bohr and Mottleson Approximation	8
2.6	Diagonalisation	10
3	Procedure	12
4	Results	13
4.1	Moments Of Inertia	13
4.2	Energy Spectrum	14
4.3	Probability	18
5	Conclusion	22
6	Acknowledgements	23

1 Introduction

Since the early days of nuclear physics, the study of rotational motion as a mode of excitation has played a vital role and been an important testing ground for many of the general ideas on nuclear dynamics [1]. The collective rotational motion of nuclei can only be observed for non-spherical equilibrium shapes, *i.e.* deformed nuclei, since the orientations with respect to an axis of symmetry are quantum-mechanically indistinguishable for the spherical case. Nuclei with permanent deformed shapes are shown to exist in regions far from filled neutron and proton shells (Figure 1). The most important deformations around the ground states of nuclei are known to be of axial-symmetry, where rotations can occur about either of the two axes perpendicular to the symmetry axis, which have equal moments of inertia [2]. Rotation about the symmetry axis are once again quantum-mechanically impossible. At high spins, however, one expects a considerable deviation from axial symmetry, which is naturally caused by the Coriolis and centrifugal forces. Such triaxial shapes will rotate with three distinct moments of inertia about any of the principle axes. For a rigid-body in classical mechanics, rotations about the axis with the largest moment of inertia are energetically favoured, however, in quantum mechanics, fluctuations in the non-quantised components of angular momentum produce a non-uniform 3-dimensional motion, known as wobbling.

Nuclear wobbling motion was originally predicted by Aage Bohr and Ben Mottleson 30 years ago in the context of the macroscopic rotor model [3]. The first experimental evidence for such a phenomenon was published in 2001 for ^{163}Lu [4]. Subsequent possible wobbling excitations were then reported in other Lu isotopes [5], but as yet none have been observed for even-A nuclei. Despite the experimental evidence to support the wobbling motion theory, there are a number of unresolved issues with the original Bohr and Mottleson model. The first quantum theory dealing with 3D rotations of very high spin nuclei predicted that a triaxial shape would exhibit harmonic excitations, however, strong anharmonicity has been observed experimentally.

One solution to this discrepancy was suggested by Matsuzaki and Ohtsubo in their tilted-axis cranking model [6]. Matsuzaki *et al* calculated the energy of the rotating

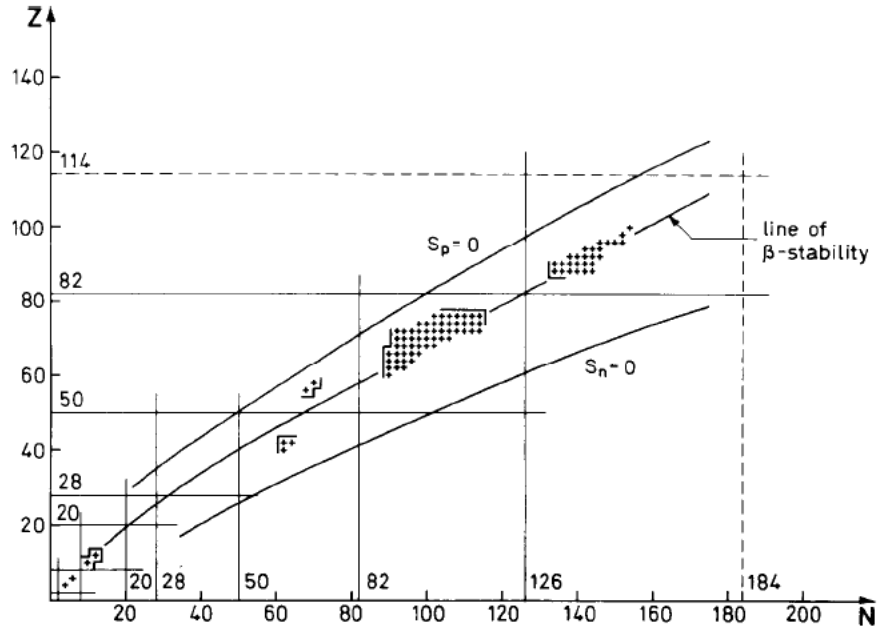


Figure 1: Regions of known deformed nuclei. Vertical and horizontal lines indicate closed shells

nucleus with respect to the tilt-angle of the total angular momentum vector. It was found that as angular momentum increases, the harmonicity of the rotation breaks down, until some critical value is reached and a phase transition occurs. In this transition, the rotational modes start to compete with each other, creating a quantum mechanical superposition of states. This occurs between the principle-axis of the quadropole deformation and some tilted-axis of rotation. Phase transition is a widely used concept amongst the physics community, with many applications for infinite systems such as superconductivity, however, its manifestation is not so clear for finite systems such as nuclei.

This project reviews the fundamental theory of rotational motion in nuclei, with particular emphasis on the Bohr/Mottleson model and a semi-classical wobbling model derived for anharmonic motion [7]. An existing piece of computer code is utilised to generate results on nuclear wobbling motion. The results are analysed, comparing them to the underlying theory and experimental observations.

2 Background Theory

2.1 Rotational Motion

For a pure liquid drop model it is possible for only those nuclei with a spherical surface to be in a stable equilibrium. However, as a consequence of quantum mechanics (shell effects) it is possible to have certain nuclei with stable ground state deformations. These states exhibit rotations, whose dynamics can be described collectively in terms of surface parameters in the laboratory frame. The kinetic energy of a classical rotating body in 3D is defined in terms of its angular momentum, L , where ζ_i is the moment of inertia:

$$E = \sum_{i=1}^3 \frac{L_i^2}{2\zeta_i} \quad (1)$$

The rotational energy is defined in the body-fixed system (*i.e.* intrinsic frame), where the moments of inertia, ζ_i , are functions of the deformation parameters β and γ about the fixed axes.

2.2 Deformation Parameters

Generally nuclei are assumed to have a sharp surface when considering their properties in the liquid drop model. Although this assumption is not strictly true, it allows the nuclear surface to be parameterised in a simple way. One such way is by considering the length of the radius vector pointing from the origin to the surface for a fixed volume, where R_0 is the radius of a sphere with the same volume [8]:

$$R(\Theta, \phi) = R_0 \left(1 + \alpha_{00} + \sum_{\lambda=1}^{\infty} \sum_{\mu=-\lambda}^{\lambda} \alpha_{\lambda\mu} Y_{\lambda\mu}(\Theta, \phi) \right) \quad (2)$$

For a quadropole shape ($\lambda=2$, where deformations are approximately ellispoidal), μ has integer values between $-\lambda$ and λ , so there are generally five parameters that are required to describe such quadropole deformations. However, not all of these parameters describe the shape of the liquid drop. Three of them determine only the orientation in space and correspond to the Euler angles, which are transformed into the body-fixed frame characterised by three axes (1,2,3). These coincide with the principle axes of the mass distribution of the body. The two remaining parameters can be defined in terms of β

and γ deformations. β deformations involve axially symmetric oscillations, whereas γ deformations destroy axial symmetry. γ values of 0° , 120° and 240° correspond to prolate spheroids with symmetry along the 3, 1 and 2 axes respectively. Values of 180° , 300° and 60° lead to oblate shapes with the same symmetry axes and values that are not multiples of 60° correspond to triaxial shapes [8]. Due to discrete symmetries about the three axes, the interval $0^\circ < \gamma < 60^\circ$ is therefore sufficient to describe all quadropole shapes.

2.3 Moment Of Inertia

Moment of inertia is the rotational analog to mass for linear motion and can be defined as a function of the two quadropole deformation parameters, β and γ [8]. It also describes the type of motion of the collective system. Two extremes for the motion of a rotating nucleus are irrotational flow and the rigid body rotor. Irrotational flow describes a system in which the nucleons are weakly bound. There is no friction in the core and therefore it does not rotate, whereas the outside nucleons will rotate (figure 2). For a system which exhibits irrotational flow, the quadropole deformation parameters are related to the moment of inertia, ζ_{irr} , by:

$$\zeta_{irr} \propto \beta^2 \sin^2 \left(\gamma - \frac{2\pi}{3} \kappa \right) \quad \kappa = 1, 2, 3 \quad (3)$$

The alternative is a rigid body rotor, where the nucleons are tightly bound and the system rotates as a whole. This differs from the moment of inertia for a system exhibiting irrotational flow with the same deformation by:

$$\zeta_{rig} \propto \left[1 - \sqrt{\frac{5}{4\pi}} \beta \cos \left(\gamma - \frac{2\pi}{3} \kappa \right) \right] \quad (4)$$

A limit is applied for a range of small β values in order to preserve the fixed volume condition of the liquid drop model, but generally the moments of inertia found experimentally fall between the two extremes, with $\zeta_{irr} < \zeta_{exp} < \zeta_{rig}$. This suggests that the flow structure within nuclei is neither that of irrotational flow or a rigid body and is intermediate of the two cases. For the purpose of this project these two limiting cases are examined. The total moment of inertia is considered as the sum of the individual components with respect to each principle axis, with rotations about the axis with the highest component being energetically favoured.

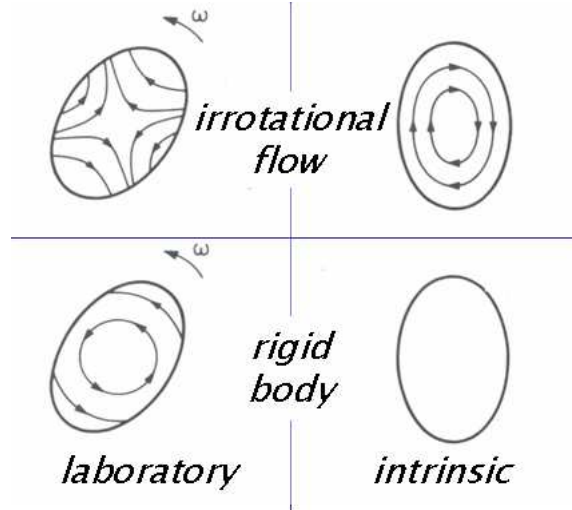


Figure 2: Rotation of an irrotational and rigid body in the laboratory and intrinsic frame

2.4 Macroscopic Quantum Rotations

In a quantum mechanical description of rotational motion, based on the assumption that the system has no internal structure, the kinetic energy and angular momentum are replaced by the Bohr Hamiltonian, \hat{H} , and total angular momentum operator, \hat{I} . \hat{I}^2 is a conserved quantity and therefore commutes with the Hamiltonian ($[\hat{H}, \hat{I}^2] = 0$):

$$\hat{H} = \sum_{i=1}^3 \frac{\hat{I}_i^2}{2\zeta_i} \quad (5)$$

For the case of axial symmetry (for example about the 3-axis), the condition $\zeta_1 = \zeta_2 > \zeta_3$ applies, where the wavefunction is an eigenfunction of the angular momentum operator, I_3 . Any rotation about this axis produces only a phase, which has the same wavefunction and energy as the ground state, making it indistinguishable from the original one. It is therefore necessary to consider rotations which occur away from the symmetry axis. For a triaxial rotor, the components of the moment of inertia, ζ_i , take a different value for each principle axis. Generally, the inequality $\zeta_1 > \zeta_2 > \zeta_3$ is supposed [3], however in this case each angular momentum component, \hat{I}_i , does not commute with the Hamiltonian ($[\hat{H}, \hat{I}_i] \neq 0$).

In order to consider a model for a triaxial rotor, which exhibits wobbling motion, the Hamiltonian can be decomposed into two terms:

$$\hat{H} = \frac{I(I+1)}{2\zeta_1} + \hat{H}_w \quad (\hbar = 1) \quad (6)$$

The first term relates to a lowest energy, or ground state for given I , where the first axis is quantised and the condition $\zeta_1 > \zeta_2 > \zeta_3$ applies. This is termed as the yrast state. The second term is a perturbation caused by contributions from the non-quantised moment of inertia components, which serves to increase the energy of the system into excited states. \hat{I}_2 and \hat{I}_3 are therefore the dynamical variables. This is the wobbling component of the Hamiltonian, \hat{H}_w , and is given as:

$$\hat{H}_w = \frac{1}{2} \left(\frac{1}{\zeta_2} - \frac{1}{\zeta_1} \right) \hat{I}_2^2 + \frac{1}{2} \left(\frac{1}{\zeta_3} - \frac{1}{\zeta_1} \right) \hat{I}_3^2 \quad (7)$$

In order to evaluate the energy spectrum, a quantisation of the classical Hamiltonian must be carried out and the energy eigenvalue equation solved:

$$\hat{H}\Psi = E\Psi \quad \Rightarrow \quad \sum_{i=1}^3 \frac{\hat{I}_i^2}{2\zeta_i} \Psi = E\Psi \quad (8)$$

The Hamiltonian possesses both rotational symmetry and a discrete intrinsic symmetry within the system that arises from a rotation by π about the i th axis. The eigenstates of the Hamiltonian are labelled by the total angular momentum, I , and the rotational symmetry is confirmed through examination of the commutation relation $[\hat{H}, \hat{I}^2] = 0$, where $\hat{I}^2 = \sum \hat{I}_i^2$. There are then two ways to solve this problem.

2.5 The Bohr and Mottleson Approximation

Originally, Bohr and Mottleson used approximation methods to solve the eigenvalue equation and predict a harmonic energy spectrum. Since the majority of the rotational motion is said to occur along the first axis, where \hat{I}_2 and \hat{I}_3 are the dynamical variables, the condition $I = \langle \hat{I}_1 \rangle \gg 1$ is introduced. This makes the model analogous to classical wobbling motion, since deformed shapes are most likely to occur at high spin, with the majority of angular momentum being carried along one of the principle axes. K is defined as the eigenvalue of \hat{I}_1 and not a good quantum number (due to its non-commutability). The quantum state of wobbling is described by the wavefunction and is written as a superpo-

sition in terms of sets, where $|C_K|^2$ is the probability for nuclear rotations to be along the 1-axis and therefore relates to the amplitude of wobbling motion:

$$|\Psi_I\rangle = \sum_K C_K |IK\rangle \quad \sum |C_K|^2 = 1 \quad (9)$$

The expectation value is expressed with respect to the state given by the above equation, where the following condition must be satisfied:

$$|C_I|^2 \gg \sum_{K \neq I} |C_K|^2 \quad (10)$$

From the normalisation condition $\sum_{K=-I}^I |C_K|^2 = 1$, the expression $|C_I|^2 \approx 1$ is implied. Since the quantised component of angular momentum, \hat{I}_1 and the Hamiltonian, \hat{H} do not commute it is necessary to consider commutation relations between \hat{I}_1 and the operator, \hat{I}_\pm (Appendix A). These are known as raising and lowering operators, and are generally used for harmonic oscillators, where:

$$\hat{I}_\pm = \hat{I}_2 \pm i\hat{I}_3 \quad \Rightarrow [\hat{I}_+, \hat{I}_-] = 2\hat{I}_1 \quad (11)$$

The commutation relation $[\hat{I}_+, \hat{I}_-] = 2\hat{I}_1 \approx 2\hat{I}$ is obeyed, and can therefore be treated in terms of boson creation and annihilation operators, where:

$$a = \frac{\hat{I}_+}{\sqrt{2I}} \quad a^* = \frac{\hat{I}_-}{\sqrt{2I}} \quad (12)$$

This produces the relationship:

$$[a, a^*] = 1 \quad (13)$$

In a particle analogy of motion, this says that increasing the angular momentum by one unit produces a boson. In terms of a wobbling motion we can relate this to the production of a quantised unit of vibration called a phonon. The resulting energy spectrum can be expressed in the form:

$$E(n, I) = \frac{\hbar^2}{2\zeta_1} I(I+1) + \left(n + \frac{1}{2}\right) \hbar\omega_{wob} \quad (14)$$

$$\Rightarrow \hbar\omega_{wob} = \hbar\omega_{rot} \sqrt{\frac{(\zeta_1 - \zeta_2)(\zeta_1 - \zeta_3)}{\zeta_2\zeta_3}} \propto I_1 \quad (15)$$

In these expressions, n is the number of wobbling phonons and $\hbar\omega_{rot} = \frac{I}{\zeta_1}$. Increasing the angular momentum, I , corresponds to adding rotational energy to the nucleus, where the nuclear excited states form a sequence known as a rotational band. This linear increase of energy within each band is typical of a system exhibiting harmonic oscillations, where the second term relates to the excitation above the yrast state and therefore the extent of wobbling.

2.6 Diagonalisation

The second way to solve the eigenvalue equation is by exact diagonalisation. It is written in the following form:

$$\sum_{K=-I}^I C_K \hat{H} |IK\rangle = E \sum_{K=-I}^I C_K |IK\rangle \quad (16)$$

This expression can then be simplified by using orthogonality conditions:

$$\langle IK' | IK \rangle = \delta_{K'K} \quad (17)$$

The eigenvalue equation becomes:

$$\sum_{K=-I}^I C_K \langle IK' | \hat{H} | IK \rangle = E \sum_{K=-I}^I \langle IK' | IK \rangle C_K \quad (18)$$

$$\Rightarrow \sum_{K=-I}^I \hat{H}_{K'K} C_K = E C_K \quad (19)$$

The expression $\langle IK' | \hat{H} | IK \rangle$ is a matrix which must be diagonalised in order to determine the eigenvalues of the Bohr Hamiltonian. A matrix, A , is said to be diagonalised if there exists an inverse of a matrix, P , such that $P^{-1}AP$ is a diagonal matrix. The eigenvalues are then simply the diagonal matrix elements.

For the case $I = 1$, the Hamiltonian is a 3x3 matrix, since both K and K' run in integer steps from $-I$ to I . The eigenvalue equation can then be represented by:

$$(H - EI)\underline{C}_K = 0 \quad (20)$$

The non-trivial solution to this expression occurs if $|H - EI| = 0$, which is possible to solve analytically for low values of I . However, in a realistic situation spin states can be observed up to $I \approx 80\hbar$. Since the Hamiltonian matrix in the eigenvalue equation has $2I + 1$ dimensions, solutions are only obtainable numerically for cases where $I \gg 1$.

Due to the discrete point group symmetry possessed by the Hamiltonian in this model two types of solution to the eigenvalue equation for any given total angular momentum are possible. One solution contains the energy eigenvalues for the even K -values and is classed as type 1 wobbling, whereas the other solution contains the values for odd K -values and is defined as type 2 wobbling. The type which possesses the lowest energy, or yrast state depends on the value of I . When I has even values, type 1 wobbling is lower in energy than type 2 and when I is odd, the type 2 solution contains the yrast state (Appendix B). A signature function can therefore be introduced, where $r = (-1)^I$. This signature is a good quantum number, so wobbling states can be labelled by I and r .

The code used for the purpose of this project calculates energy eigenvalues of the perturbed part of the Hamiltonian only. It allows the user to specify the total angular momentum, signature and deformation parameters. Diagonal elements, where $K' = K$, are given as [9]:

$$\langle IK | \hat{H}_w | IK \rangle = \frac{1}{4} \left(\frac{1}{\zeta_2} + \frac{1}{\zeta_3} - \frac{2}{\zeta_1} \right) I(I+1) - K^2 \quad (21)$$

The off-diagonal matrix elements are:

$$\langle IK' \pm 2 | \hat{H}_w | IK \rangle = \frac{1}{8} \left(\frac{1}{\zeta_3} - \frac{1}{\zeta_2} \right) \sqrt{(I \pm K)(I \pm K - 1)(I \mp K + 1)(I \mp K + 2)} \quad (22)$$

Diagonalisation is carried out numerically to obtain eigenstates in the form of equation 7. Due to spontaneous symmetry breaking arguments, the condition $K > 0$ is applied to $|IK\rangle$, where a level sequence with $I = 0, 2, 4, \dots$ arises due to the discrete symmetry from rotations of π about a principle axis.

3 Procedure

This project involves using an existing piece of computer code based on the Bohr/Mottleson model for collective rotational motion. The Hamiltonian is decomposed into two terms with a constant yrast term and perturbation, which relates to the wobbling component [7]. The model is based on exact diagonalisation of this Hamiltonian matrix. The user sets values for the spin state of the nucleus, phonon number, signature and deformation parameters and then chooses either the rigid body or irrotational flow case to represent each component of the moment of inertia. The matrix $\langle IK' | \hat{H}_w | IK \rangle$ is specified with dimensions $I + 1$ (and not $2I + 1$ due to the spontaneous symmetry breaking as discussed previously). The diagonal and off-diagonal components are filled using equations 18 and 19, where the result is a symmetric matrix. The program then utilises a standard mathematical function to diagonalise the matrix. The diagonal components of this matrix are the eigenvalues that form the energy spectrum and the eigenvectors for each value of K in any given spin state, I , are of the form of equation 7. The square of the resultant wavefunction relates to the probability for the given rotor to be aligned along the quantised first axis. Any deviation from this axis corresponds to a wobbling motion.

Initially, a rigid body moment of inertia was chosen to represent the system for a spin state of $I = 41\hbar$ with a negative signature to produce the lowest energy levels, $\beta = 0.4$ and phonon number of 1. The program was run for γ -values between -60 and 60° . The code was then adapted to allow for an irrotational flow moment of inertia under the same set of conditions, and the results for each case compared.

4 Results

4.1 Moments Of Inertia

Figures 3 and 4 show how each component of the moment of inertia, ζ_i , depends on the deformation parameter γ for an irrotational flow and a rigid body. These dependencies are normalised to 1 about $\gamma=0^\circ$, since the relationships shown in eqns 3 and 4 will also contain a number of constants relating to the nuclear mass and radius. γ -values of -60° , 0° and 60° relate to nuclei with deformed shapes of axial symmetry (*i.e.* where two of the moments of inertia are equal, as seen in the figures). All other values produce triaxial shapes. It can be seen that in the region of $\gamma=-60^\circ$ to 0° the highest component of the moment of inertia is ζ_2 for the irrotational case and ζ_1 for the rigid body. This means that the majority of the rotational motion in this region will occur along the second and first, (or shortest) principle axes respectively, with fluctuations most likely to occur along the 1- and 2-axes. In the $\gamma=0^\circ$ to 60° range, ground state rotations occur along the first-axis for irrotational flow and the intermediate-axis for the rigid body. Since the Bohr/Mottleson model choses the 1-axis for quantisation, only the 0° to 60° region for an irrotational flow case relates to ground state rotations. Similarly, the $\gamma=-60^\circ$ to 0° for the rigid body case relates to the ground state, (*i.e.* where ζ_1 is largest). Other regions relate to excited states.

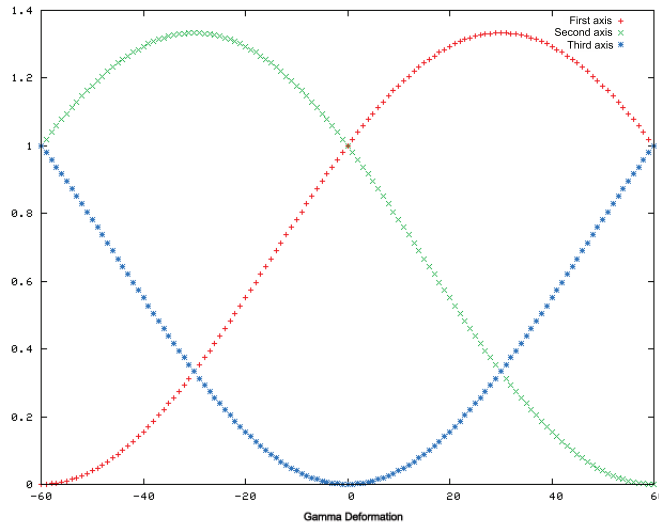


Figure 3: Dependence of ζ_i on γ -deformation for the case of irrotational flow

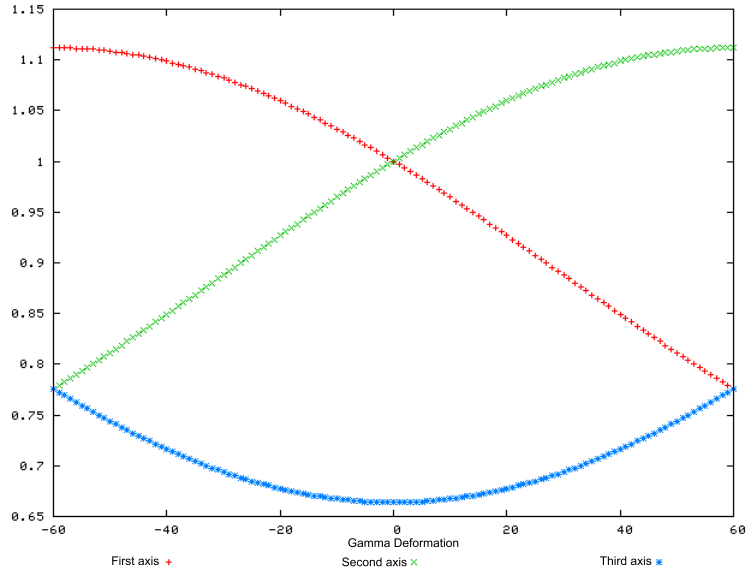


Figure 4: Dependence of ζ_i on γ -deformation for the case of a rigid body

4.2 Energy Spectrum

Figure 5 shows the energy eigenvalues of the first angular momentum component as a function of γ -deformation for the ground and successive states in the rotational band due to a rigid body flow structure. Some harmonicity is exhibited in the spectrum, however, where the energy levels move closer together indicates the anharmonicity in the system. The range $\gamma = -60^\circ$ to 0° indicates the region where rotations are energetically favourable along the shortest axis (1-axis), where γ -values of -60° and 0° represent deformations with axial symmetry. We can therefore look to these regions for some understanding of the underlying physics.

At $\gamma = -60^\circ$, moments of inertia have equal values along the 2- and 3-axes, with a maximum along the quantised axis. This indicates that rotations will predominantly occur along the first axis, with fluctuations along the 2- and 3-axes contributing equally. As the energy increases above the yrast state there is a larger contribution from the perturbed Hamiltonian, and therefore a greater amplitude of wobbling. The energy separation gradually decreases as the fluctuations from the non-quantised components increase, until a phase transition occurs into rotations about the intermediate axis.

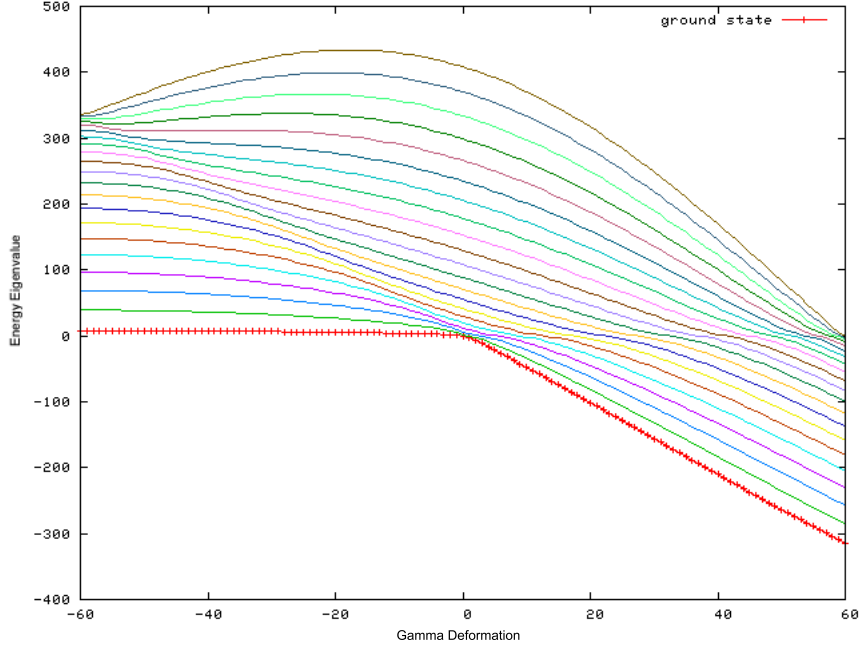


Figure 5: Anharmonic energy spectrum for a rigid body

At $\gamma=0^\circ$, moment of inertia has equal components along the 1- and 2-axes. Rotations would therefore be expected to occur along these principle axes equally, implying some phase transition between the two states at low excitations. In this region the anharmonicity is shown to occur around the ground (lowest energy) and first few successive states, suggesting a transition between rotations about the two axes.

The anharmonic region appears to follow a linear relationship as a function of γ . As the γ -value increases from -60° to 0° the harmonic break-down occurs at lower energies. This region represents a phase transition from the shortest, quantised axis to rotations predominantly around the second axis. As γ increases this transition occurs closer to the yrast energy. This makes sense since the first moment of inertia component decreases in magnitude as the axial symmetric deformation at $\gamma=0^\circ$ is approached. At this value, both the first and second axes have an equal contribution, therefore rotations can occur equally along them without excitation.

The 0° - 60° γ -range represents an excited mode of rotation, since motion is energetically favoured around the second axis. Energy eigenvalues are shown to decrease rapidly as γ

increases, with a larger degree of anharmonicity. All of these excitations enter negative energy values, which is reasonable since we are only considering the perturbed part of the Hamiltonian. In reality the energy of the yrast state must be added to each of these values, however, the sudden decrease in energy eigenvalues suggests that lower energy states are preferred (*i.e.* rotations along the intermediate axis).

The ground state rotation over the full range shows a constant energy through to $\gamma=0^\circ$. The energy value is just above zero, suggesting that there is minimal contribution from the perturbed Hamiltonian and therefore no fluctuations from the non-quantised axes. This suggests that there is no (or very small amplitude) wobbling just above the yrast state. At $\gamma=0^\circ$ the energy starts to drop below zero, representing the transition from rotations along the quantised axis, to the second axis. There would therefore be a very large wobbling amplitude. beyond this, rotations occur along the second axis, with contributions from the first axis decreasing rapidly.

It should be noted that although the y -axis of this figure represents the energy eigenvalues, it is a unitless quantity at the present stage since mass and radius values for specific nuclei, which contribute to the moment of inertia have not been accounted for.

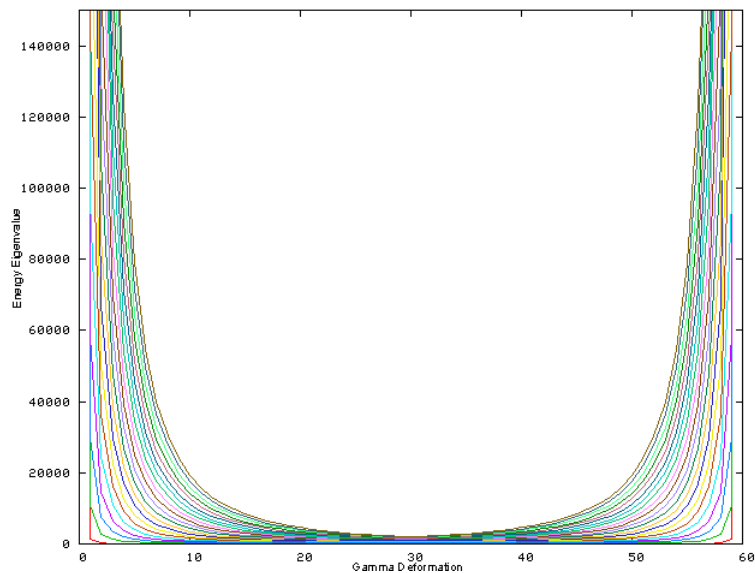


Figure 6: Energy spectrum for irrotational flow

Figure 6 shows a similar energy spectrum for the case of irrotational flow. Only the region where first axis rotations are favoured is shown ($\gamma=0^\circ-60^\circ$). It can clearly be seen that the function is symmetric about $\gamma=30^\circ$, which is sensible due to the fact that the moment of inertia function (figure 3) is also symmetric for this region. This allows us to concentrate on just the $\gamma=0^\circ-60^\circ$ region. As γ approaches 0° the energy eigenvalues in the spectrum increase rapidly by several orders of magnitude. This suggests that as the nucleus approaches axial symmetry, more energy is required to rotate it about the first axis, until at $\gamma=0^\circ$, infinite amounts of energy are required, and therefore rotations are impossible.

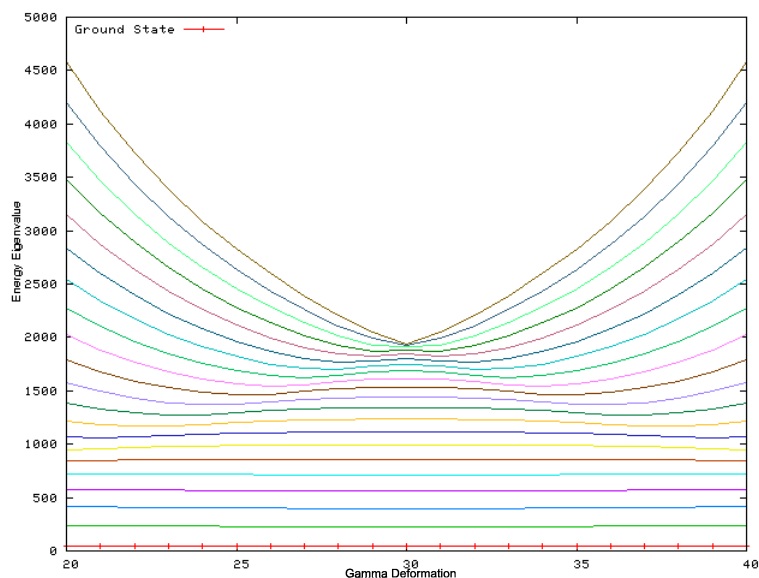


Figure 7: Energy spectrum for irrotational flow over the $\gamma = 20 - 40^\circ$ range

Figure 7 now shows the $\gamma=20^\circ$ to 40° range more clearly, where the harmonicity of the system can be explored. Again we can look at just the 20° to 40° range for some understanding. In the lowest energy state there appears to be little or no contribution from the perturbed part of the Hamiltonian, so just above the yrast state there is only a small wobbling amplitude. Initially, as the energy levels increase the separation between them is almost constant, representing a harmonic system, however, this starts to break down, once again representing large wobbling amplitudes and a phase transition. As the deformation of the nucleus moves away from axial symmetry the initial convergence of the energy levels, and therefore the transitions occur at higher energies for increasing γ -

values up to 30° . $\gamma=30^\circ$ corresponds to the maximum contribution from the first moment of inertia component and therefore the lowest energies of the system. However, although these levels do not relate directly to energies with conventional units, they are still several magnitudes larger than the energies calculated for a rigid body. This is due to the fact that the moment of inertia components have lower values than for a rigid body.

4.3 Probability

Figure 8 shows $|\Psi|^2$ or probability for first axis rotations as a function of each K -eigenvalue for an angular momentum value of $I = 41\hbar$, negative signature and rigid body flow structure. This probability distribution is represented for each γ -value from -60° to 60° . It can clearly be seen that there are at least two types of function present in the spectrum, including a sharp main peak with a probability close to 1, and a smaller peak at lower K -values (where K is the eigenvalue of \hat{I}_1). The second type of peak has maximums with probabilities of $\sim 20\%$ over a wide spread of eigenvalues. Once again we must turn to our knowledge of the moment of inertia as well as the energy spectra to understand these functions.

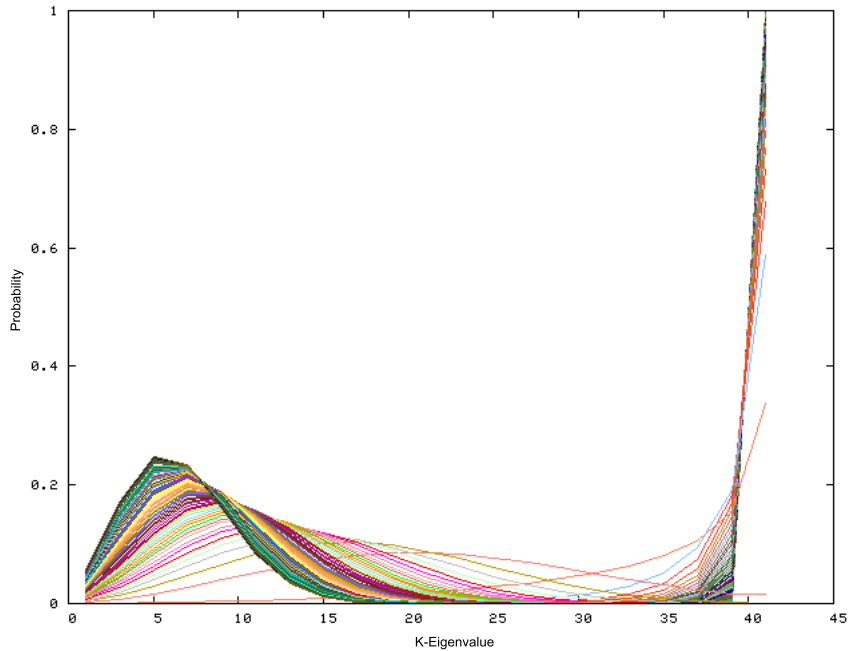


Figure 8: Probability spectrum as a function of the K eigenvalue for each γ -deformation

First, lets consider the -60° to 0° γ -range, where ground state rotations occur along the

quantised first axis. Figure 9 shows the probability functions for $\gamma=-60^\circ$ and $\gamma=0^\circ$. At -60° there is a sharp peak up to 100% at $K=41$, with negligible probability for rotations to occur in any other state. The high K -value state relate to a situation where virtually all of the total angular momentum is aligned along the first principle axis, so at -60° there are few contributions from the other two moment of inertia components and therefore only a small wobbling amplitude.

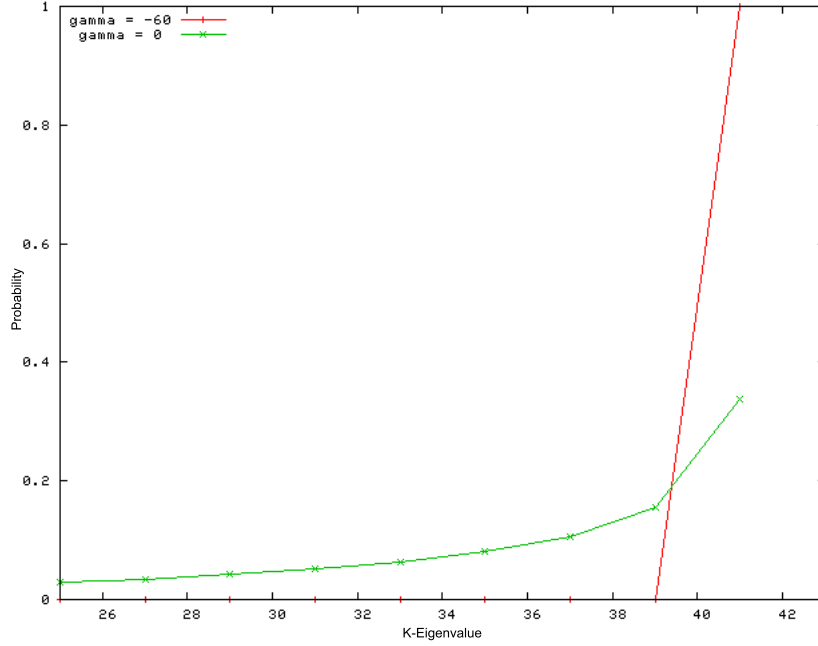


Figure 9: Probability distribution as a function of the K eigenvalue for $\gamma=-60^\circ$ and 0°

At $\gamma=0^\circ$ the function shows a more shallow rise with increasing K -value and a maximum probability of $\sim 40\%$ at $K=41$. There is also a significant probability for rotations to be in successive states (where the area under the function relates to a 100% probability). This means that there is a 40% probability for the nucleus to be in a state with no (or very low amplitude) wobbling. As the K -value decreases, contributions from the two other principle axes begin to play a role, with a decreasing probability or larger amplitude wobbling.

These functions are easily understood from consideration of the moment of inertia relationship for a rigid body (figure 4). Since components ζ_1 and ζ_2 have equal contributions at $\gamma=0^\circ$, it would be expected for rotations to occur along the two principle axes

equally, with some contribution from a phase transition between the two. At 60° , ζ_1 has the largest component and as expected there are very few contributions from the other components. Between these two limiting situations the probabilities have intermediate functions (Appendix C).

If we now consider the $\gamma=0^\circ$ to 60° range a different type of function emerges. In this region there is no probability for rotations to be aligned along the quantised axis in the ground state and first few successive states ($K=41-30$). Beyond this, as the K -eigenvalue (and therefore the contribution from I_1 to the total angular momentum) decreases, there is an increasing probability for rotations to be along the 1-axis. This probability then decreases once more as K approaches 0. Since the largest moment of inertia contribution is ζ_2 in this range, it would be expected that there are no (or very few) contributions from ζ_1 in the ground state. As the nucleus enters excited states, however, it would be expected that there would be larger contributions from the 1-axis (since it has the second largest moment of inertia), until a phase transition occurs to rotations along this axis. The maximum probability for rotations along the first axis is $\sim 20\%$ at $K = 5$, which relates to large amplitude wobbling.

Figure 10 shows the full probability distribution of rotations along the 1-axis as a function of K -eigenvalue for irrotational flow. Once again, several types of function emerge, with two sharp sets of peak at 100% probability and a more shallow peak with a wider spread over the K -values. Figure 11 shows the functions for $\gamma=30^\circ$ and 60° . At 30° there is a 100% probability for rotations to occur along the first axis at $K=41$. Since ζ_1 has the largest contribution, with ζ_2 and ζ_3 having equal contributions, this result is expected. At 0° and 60° there are two equal moments of inertia with equal contributions. It is therefore expected that for both of these cases rotations occur along both principle axes equally. In the ground state ($K=41$) this appears to be the case, with rotations occurring along the quantised axis $\sim 40\%$ of the time. At increasingly excited states (decreasing K) there is still a finite probability for rotations along this axis, although it decreases rapidly, relating to larger wobbling amplitudes and eventually a transition to another principle axis. Intermediate values between 0° and 60° can be seen in Appendix C.

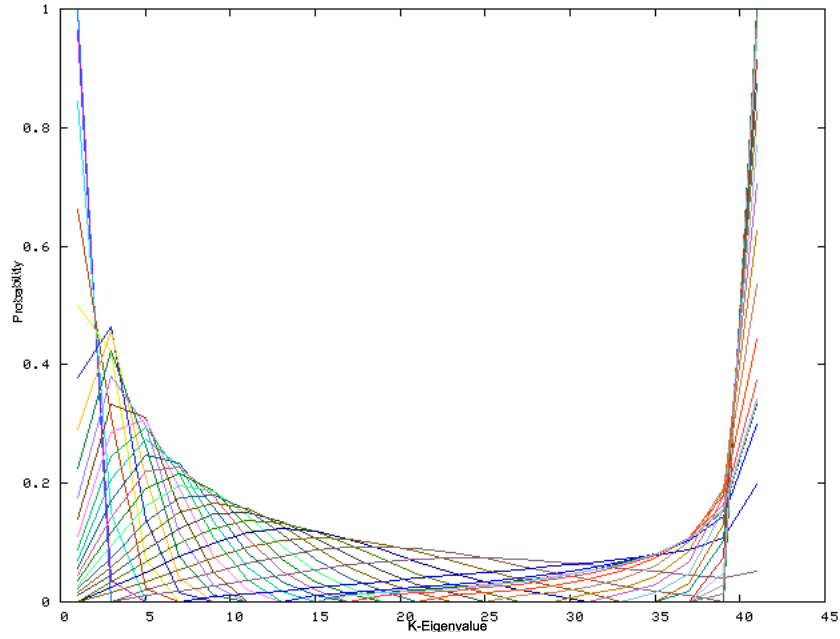


Figure 10: Probability distribution as a function of the K eigenvalue

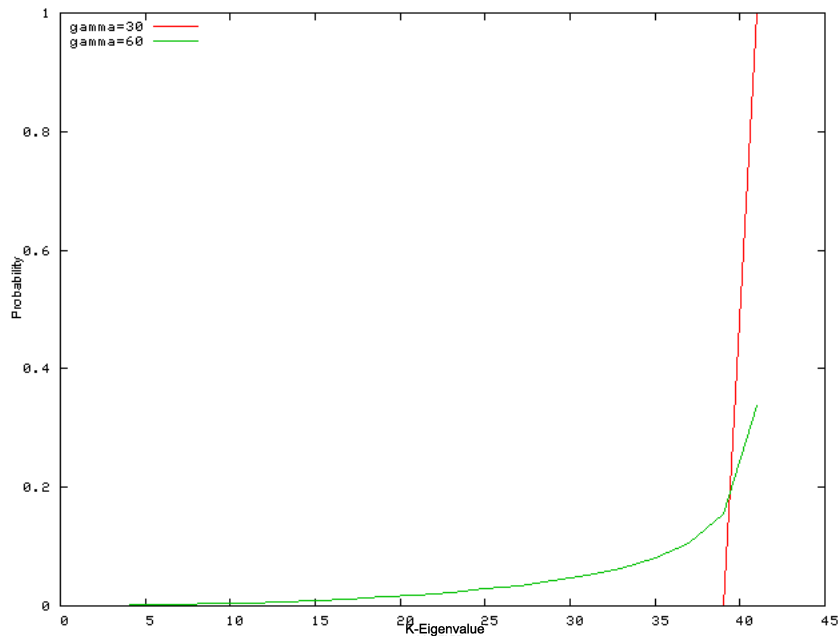


Figure 11: Probability distribution as a function of the K eigenvalue for $\gamma=30^\circ$ and 60°

As the γ -range is extended to include the full -60° to 60° region (figure 10) another sharp peak can be seen. This occurs at $\gamma=-30^\circ$, where the ζ_3 component has the largest contribution. As expected, there is no probability for rotations along the first axis in the

ground state, however, in the most excited states a transition occurs and rotations are fully aligned along the 1-axis. In the ranges -60° to -30° and -30° to 0° the wider, more shallow peaks emerge, which relate to probabilities for first axis rotations of $\sim 30\%$ at high excitations. There will be high amplitude wobbling in these regions, which decreases as the K -eigenvalue increases.

5 Conclusion

This project has reviewed some of the basic theory of rotational motion in nuclei with aim to understanding the concepts of wobbling motion. An existing piece of computer code was utilised based on exact diagonalisation of the perturbed part of the Hamiltonian, which arises due to contributions from the moment of inertia along the non-quantised axes. The energy spectrum of the rotating system is assessed by solving the time-independent Schrodinger equation with respect to the chosen quantised axis. Standard mathematical functions are then utilised to diagonalise the Hamiltonian matrix.

For a triaxial rotor, γ -deformations between -60° and 60° were explored for both a rigid body and irrotational flow structure. Anharmonic energy spectra were produced, similar to those described by recent experimental data. However, in this model only the collective, or macroscopic properties of the system were considered, where there was assumed to be no internal structure of the nucleus. In reality, the microscopic properties, such as pairing and other shell effects must also be considered before a direct comparison can be made with experimental data. Future work and development is necessary for a full understanding of this mode of excitation and to resolve the discrepancies which exist between the original Bohr and Mottleson model and the published experimental evidence.

6 Acknowledgements

The author would like to thank Dr. M. Oi for his supervision and guidance through this project, and Julian Fletcher for his useful discussion and advice.

References

- [1] Aage Bohr *Rotational Motion In Nuclei* The Niels Bohr Institute and NORDITA Rev. Mod. Phys. **48**, 365(1976)
- [2] Kenneth S. Krane, *Introductory Nuclear Physics*, Second edition, John Wiley & Sons, Inc. 1987. ISBN 0-471-80553-X
- [3] Aage Bohr & Ben R. Mottleson *Nuclear Structure Vol. II: Nuclear Deformations* World Scientific. 1998 ISBN 9810231970
- [4] S. W. Odegard *et al Evidence for the Wobbling Mode in Nuclei* Phys. Rev. Lett. **86**, 5966(2001)
- [5] D. R. Jensen *et al Evidence for Second-Phonon Nuclear Wobbling* Phys. Rev. Lett. **89**, 142503(2002)
- [6] Masayuki Matsuzaki & Shin-Ichi Ohtsubo *Instability of Nuclear Wobbling Motion and Tilted Axis Rotation* Phys. Rev. C **69**, 064317(2004)
- [7] Makito Oi *Semi-Classical and Anharmonic Quantum Models of Nuclear Wobbling Motion* Phys. Lett. B, 634, 30(2006)
- [8] P. Ring & P. Schuck *The Nuclear Many Body Problem* Third Edition, Springer. 2004 ISBN 3-540-21206-X
- [9] Makito Oi *Effects of K-Mixing in the Wobbling Model* University of Surrey. 2005
- [10] Makito Oi & Julian Fletcher *Problems in Nuclear Wobbling Motion* J. Phys. G: Nucl. Part. Phys. **31**, S1753(2005)

Appendix A: Commutation Relations

The matrix elements for $\langle IK'|\hat{H}|IK\rangle$ need to be calculated, where the Hamiltonian is a function of the angular momentum components (eqn 7). \hat{I}_1 is defined as the quantised component, where K is its eigenvalue. Rather than work with \hat{I}_2 and \hat{I}_3 directly, it is useful to introduce raising and lowering operators, where $\hat{I}_\pm = \hat{I}_2 \pm i\hat{I}_3$. \hat{I}_+ is the lowering operator in this case as shown below:

$$\hat{I}_1(\hat{I}_+|IK\rangle) = \hat{I}_1\hat{I}_+|IK\rangle \quad (23)$$

It is useful to use the commutation relation:

$$[\hat{I}_1, \hat{I}_\pm] = \hat{I}_1\hat{I}_\pm - \hat{I}_\pm\hat{I}_1 = \mp\hbar\hat{I}_\pm \quad (24)$$

Equation 23 then becomes:

$$(\hat{I}_+\hat{I}_1 - \hbar\hat{I}_\pm)|IK\rangle = (\hbar K\hat{I}_+ - \hbar I_+)|IK\rangle \Rightarrow (K-1)\hbar\hat{I}_+|IK\rangle \quad (25)$$

$(K-1)$ is the eigenvalue of \hat{I}_+ and therefore lowers the state of the system. A similar relationship for the raising operator, \hat{I}_- , can then be obtained, which are combined into the following expression, where N is the normalisation constant:

$$\hat{I}_\pm|IK\rangle = N|IK \mp 1\rangle \quad (26)$$

The commutation relation $[\hat{I}_-, \hat{I}_+] = \hat{I}_-\hat{I}_+ - \hat{I}_+\hat{I}_- = 2\hat{I}_1$ can then be utilised in order to find the normalisation constant. This is examined from the expression $\langle IK|2\hat{I}_1|IK\rangle$, since $\hat{I}_1 \propto [\hat{I}_2, \hat{I}_3]$ (and therefore \hat{H}). In the general case this constant is found to be $N = \sqrt{I(I+1) - K(K \mp 1)}$, where $\hbar = 1$ (reducing to $N = \sqrt{2I}$ when $I = K$). The raising and lowering operators are then written as:

$$\hat{I}_\pm|IK\rangle = \sqrt{I(I+1) - K(K \mp 1)}|IK \mp 1\rangle \quad (27)$$

The relationship between \hat{I}_\pm and the angular momentum components are then applied to express the elements of the Hamiltonian matrix in the above form (equations 21 and 22).

Appendix B: Signature Discussion

The discrete symmetry possessed by the Hamiltonian in this model was discussed briefly in section 2 and a signature function introduced in order to classify the two types of solution to the eigenvalue equation. It was mentioned that for odd values of I , the type 2 wobbling solution (and therefore a negative signature) contains the yrast state of the system. This was shown in figure 5 for $I = 41$, where the lowest energy eigenvalue was just above zero. Figures 12 and 13 now show the same spin state, for just the ground state region and a negative then positive signature. It can clearly be seen that the lowest energy eigenvalue has a higher value with the positive, than for the negative signature solution.

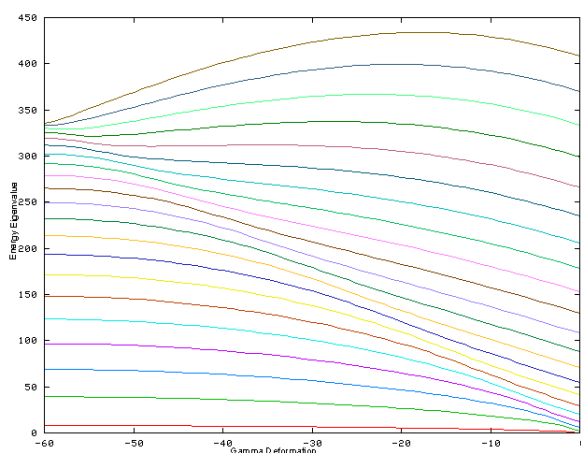


Figure 12: Energy spectrum for $I = 41$ and a negative signature

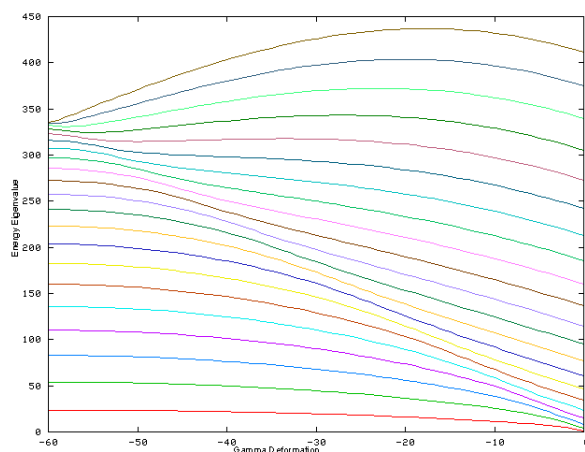


Figure 13: Energy spectrum for $I = 41$ and a positive signature

Figures 14 and 15 show similar energy spectra for the even spin state $I = 40$ with a negative and positive signature respectively. It can be seen that the solutions for the positive signature case now contain the yrast state.

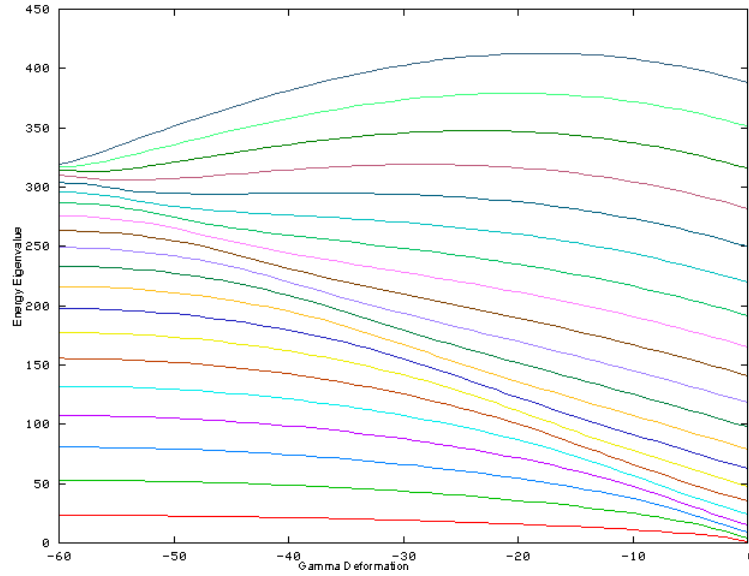


Figure 14: Energy spectrum for $I = 40$ and a negative signature

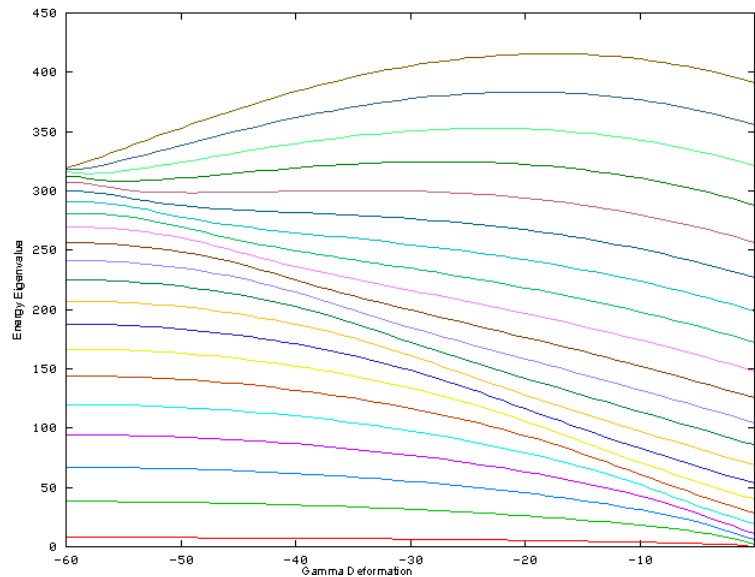


Figure 15: Energy spectrum for $I = 40$ and a positive signature

Appendix C: Additional Plots

Figure 16 shows the probability distribution for a rigid body with γ deformations between -60° and 0° .

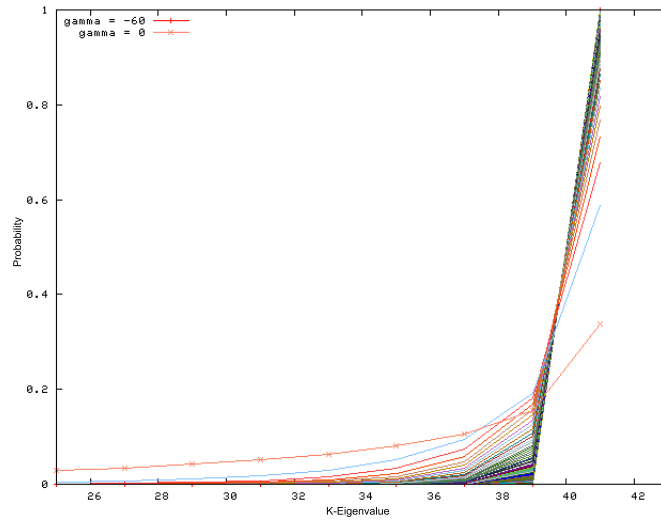


Figure 16: Probability spectrum as a function of the K eigenvalue for $\gamma=-60$ to 0°

Figure 17 shows the probability distribution for the irrotational flow case with γ deformations between 0° and 60° .

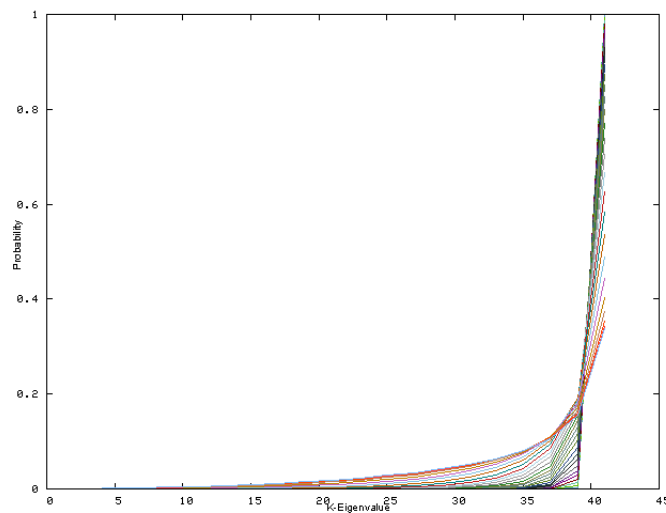


Figure 17: Probability spectrum as a function of the K eigenvalue for $\gamma=0$ to 60°